Journal of Thermal Analysis and Calorimetry, Vol. 95 (2009) 2, 387–392

MOLAR HEAT CAPACITY AND THERMODYNAMIC PROPERTIES OF CRYSTALLINE $[Nd(Glu)(H_2O)_5(Im)_3](ClO_4)_6{\cdot}2H_2O$

X.-C. Lv[1,2], *Z.-C. Tan*[2*], *X.-H. Gao*[1], *Q. Shi and L.-X. Sun*[2]

[1]School of Chemistry and Material Science, Liaoning Shihua University, Fushun, 113001 Liaoning, China
[2]Thermochemistry Laboratory, Dalian Institute of Chemical Physics, Chinese Academy of Science, Dalian 116023, China

A complex of neodymium perchloric acid coordinated with *L*-glutamic acid and imidazole, $[Nd(Glu)(H_2O)_5(Im)_3](ClO_4)_6{\cdot}2H_2O$ was synthesized and characterized by IR and elements analysis for the first time. The thermodynamic properties of the complex were studied with an automatic adiabatic calorimeter and differential scanning calorimetry (DSC). Glass transition and phase transition were discovered at 221.83 and 245.45 K, respectively. The glass transition was interpreted as a freezing-in phenomenon of the reorientational motion of ClO_4^- ions and the phase transition was attributed to the orientational order/disorder process of ClO_4^- ions. The heat capacities of the complex were measured with the automatic adiabatic calorimeter and the thermodynamic functions $[H_T–H_{298.15}]$ and $[S_T–S_{298.15}]$ were derived in the temperature range from 80 to 390 K with temperature interval of 5 K. Thermal decomposition behavior of the complex in nitrogen atmosphere was studied by thermogravimetric (TG) analysis and differential scanning calorimetry (DSC).

Keywords: *adiabatic calorimetry, glass transition, low-temperature heat capacity, $[Nd(Glu)(H_2O)_5(Im)_3](ClO_4)_6{\cdot}2H_2O$, phase transition, thermal analysis*

Introduction

Rare earth elements have many unique biochemical properties and amino acids are the basic units of biology. Since several decades of years, with great progression being made in cognition and researching of the complexes of rare earth ions with amino acids, the complexes have been used in many areas, such as fertilizer, pesticide and antibacterial agent and so on. With these applications, rare earth elements are inevitably spread into food chain, and then into the bodies of human beings. In order to obtain information about the long-term effect of rare earth elements on people and explore more extensively application of the complexes, the complexes of lanthanide ions with amino acids have been synthesised and extensively studied by a variety of methods [1–5], but only a few publications deal with thermodynamic investigation [6, 7].

In the present work, a complex of neodymium perchlorate coordinated with glutamic acid and imidazole, $[Nd(Glu)(H_2O)_5(Im)_3](ClO_4)_6{\cdot}2H_2O$, which has never been reported in other documents, was synthesized and characterized. The thermodynamic properties of the complex were studied by the adiabatic calorimetry and the DSC technique. Two special thermal phenomena were discovered and the mechanism was deduced. A precision adiabatic calorimeter was used to measure the molar heat capacity, $C_{p,m}$, of the complex. The temperature, T_{trs}, molar enthalpies, $\Delta_{trs}H_m$, molar entropies, $\Delta_{trs}S_m$, of the phase transitions and thermodynamic functions, $[H_T–H_{298.15}]$ and $[S_T–S_{298.15}]$ were derived, respectively. The mechanism of decomposition of the complex was studied by DSC and TG technique.

Experimental

Synthesis and characterization of the complex

The title complex, $[Nd(Glu)(H_2O)_5(Im)_3](ClO_4)_6{\cdot}2H_2O$, has never been reported in any other documents we have seen. The starting material was analytical reagent from the Beijing Chemical Reagent Co. Rare earth oxide (Nd_2O_3) dissolved in an excess amount of perchloric acid, and the concentration of the solution was determined by EDTA titration analysis. Then, solid *L*-glutamic acid was added to the solution of Nd^{3+} in molar ratio of Nd^{3+}: Glu=1:1. After the pH value of the reaction mixture was carefully adjusted to about 4.0 by slow addition of NaOH solution, imidazole was added. The solution was placed in a desiccator filled with phosphorus pentaoxide after a further 2 h of stirring. Cube crystals were obtained about a month later. The yields range from 30 to 35%.

An elemental analysis apparatus (Model PE-2400 II, USA) was used to measure the C, H, N of the complex and Nd was determined by EDTA titration. Found:

* Author for correspondence: tzc@dicp.ac.cn

1388–6150/$20.00

Akadémiai Kiadó, Budapest, Hungary
Springer, Dordrecht, The Netherlands

Nd (11.53%), C (13.137%), N (7.952%) and H (2.817%), which is close to the theoretical value, Nd (11.84%), C (13.790%), N (8.051%) and H (2.463%). The sample formula was determined to be $[Nd(Glu)(H_2O)_5(Im)_3](ClO_4)_6{\cdot}2H_2O$ and the purity, obtained from the EDTA titration under the same conditions was found to be 99.79%.

Infrared spectra of the complex and *L*-glutamic acid were obtained from KBr pellets at room temperature using a Bruker Tensor 27-IR spectrophotometer. Compared with the IR spectrum of *L*-glutamic acid, the ν_s (carboxyl) band of the complex shifted from 1410 cm^{-1} to higher wavenumbers (1431 cm^{-1}), which shows that the carboxyl groups of the ligand have been coordinated to the metal ion [8]. The special absorptions of $–NH_2$ shifted from 3050 to 3240 cm^{-1} ($\delta_{–NH}$), from 2750 to 2740 cm^{-1} ($\nu_{–NH}$), and from 1560 to 1562 cm^{-1} ($\delta_{NH^{2+}}$), because a hydrogen bond formed in the complex. The spectrum also shows the wide peak symmetrical resonance frequencies, $\nu_{s(N–H)}$, shifted from 3286–3425 down to 3166–3098 cm^{-1}, which is evidence of the coordination of imidazole molecules [9]. A broad absorption band for ν (hydroxyl) appearing at 3400 cm^{-1} shows the presence of water molecules in the complex.

Instrumental methods

Adiabatic calorimetry

A precision automatic adiabatic calorimeter was used to measure the heat capacities of the complex over the temperature range from 80 to 390 K. The instrument was established in Thermochemistry Laboratory of Dalian Institute of Chemical Physics, Chinese Academy of Sciences.

The structure and principle of the adiabatic calorimeter have been described in detail elsewhere [10–12]. The automatic adiabatic calorimeter consisted of a sample cell made of gold-plated copper, a miniature platinum resistance thermometer (IPRT No. 2, produced by Shanghai Institute on Industrial Automatic Meters, 16 mm in length, 1.6 mm in diameter and a nominal resistance of 100 Ω), an electric heater, the inner and the outer adiabatic shields, two sets of six-junctions chromel-constantan thermopiles installed between the calorimetric cell and the inner shield and between the inner and the outer shields, respectively, and a high vacuum can [13–15].

The effective capacity of the sample cell was 6 cm^3. Four gold-plated copper canes of 0.2 mm in thickness placed inside with an X-shape to promote heat distribution. A miniature platinum thermometer was inserted into a horizontal copper sheath soldered under the bottom. The thermometer was calibrated on the basis of ITS-90 by the Station of Low-temperature Metrology and Measurements, Academia Sinica. The resistance of the thermometer was measured by a 71/2 Digit Nano Volt/Micro ohm Meter (Model 34420, Agilent, USA). The heater wire was bifilarly wound and fixed around outside the wall of the sample cell. After the sample was loaded, the cell was sealed and evacuated. A small mount of helium gas (0.1 MPa) was introduced into the cell so as to enhance the heat transfer.

The temperature difference between sample cell and inner shield, and between inner and outer shield were monitored by two sets of thermocouples. Both shields were heated under the control of Temperature Controller (Model 340, Lakeshore, USA) and kept at the same temperatures as that of the sample cell. The electrical energy introduced into the sample cell was automatically picked up by a Data Acquisition/Switch Unit (Model 34970A, Agilent, USA). The equilibrium temperature of the cell after the energy input was measured by the 71/2 digit Nano Volt/Micro ohm meter. The energy and the temperature data were processed on line by a computer.

The heat capacity measurements were conducted by the standard procedure of intermittently heating the sample and alternately measuring the temperature. The heating rate was 0.1 to 0.4 K min^{-1}; the temperature increments of the experimental points were between 1 and 4 K; the heating duration was 10 min and the temperature drift rates of the sample cell, which was measured in an equilibrium period, were kept within 10^{-3} to 10^{-4} K min^{-1}.

Prior to the heat capacity measurement of the sample, the molar heat capacities of α-Al_2O_3, the standard reference material, were measured from 78 to 400 K to verify the reliability of the adiabatic calorimeter. The results showed that the deviation of our calibration data from those of NIST [16] was within ±0.3%.

In the present paper, the mass of $[Nd(Glu)(H_2O)_5(Im)_3](ClO_4)_6{\cdot}2H_2O$ used for the measurement was 2.7122 g, which was equivalent to 0.00196 mol based on the molar mass M=1384 g mol^{-1}.

DSC and TG

A Differential Scanning Calorimeter (DSC -141, Setaram, France) was used to perform the thermal analysis of $[Nd(Glu)(H_2O)_5(Im)_3](ClO_4)_6{\cdot}2H_2O$ from 100 to 700 K at the heating rate of 10 K min^{-1} under a purity nitrogen with liquid nitrogen as cryogen. The mass of the sample used in the experiment was 4.2 mg.

The TG measurement of the sample was carried out by a thermogravimetric analyzer (Model: DT -20B, Shimadzu, Japan) at the heating rate of 10 K min^{-1} under a purity nitrogen with flow rate of 30 mL min^{-1}. The mass of the sample used in the experiment was 7.2 mg.

Table 1 Experimental molar heat capacities of the complex from 80 to 390 K

T/K	$C_{p,m}$/J K^{-1} mol^{-1}	T/K	$C_{p,m}$/J K^{-1} mol^{-1}
81.494	576.94	161.02	934.80
85.480	586.59	164.16	950.61
88.432	600.10	167.28	964.21
91.302	613.26	170.35	978.08
94.261	626.77	173.40	993.10
97.312	640.86	176.42	1007.2
100.29	653.88	179.41	1018.9
103.20	667.28	182.37	1034.9
106.20	680.60	185.31	1051.4
109.29	696.03	188.33	1066.5
112.32	710.60	191.44	1085.2
115.29	725.32	194.51	1102.4
118.22	738.17	197.57	1120.0
121.24	751.04	200.59	1137.4
124.35	765.60	203.59	1154.5
127.42	779.71	206.57	1171.2
130.45	792.55	209.52	1186.0
133.44	810.79	212.55	1201.3
136.43	826.90	215.67	1221.0
139.51	841.25	218.76	1243.0
142.69	854.97	221.83	1268.0
145.83	869.28	224.84	1285.4
148.93	883.41	227.84	1313.1
151.99	897.38	230.76	1344.9
154.99	908.64	233.77	1370.5
239.95	1478.0	320.45	1752.9
242.94	1570.3	323.54	1772.4
245.46	3466.5	326.54	1791.9
248.65	1596.8	329.55	1803.2
252.36	1405.5	332.47	1823.7
255.39	1413.0	335.47	1843.1
258.36	1394.8	338.39	1861.6
261.12	1426.6	341.26	1882.4
264.06	1435.2	344.07	1907.2
267.04	1462.5	346.92	1941.6
270.00	1481.3	349.84	1954.4
272.94	1510.7	352.68	1992.8
275.89	1682.9	355.58	2007.0
278.69	1991.7	358.50	2036.8
281.70	1539.0	361.42	2101.7
284.84	1561.6	364.34	2199.6
287.87	1587.4	367.30	2304.9
290.91	1597.7	370.32	2204.0

Table 1 continued

T/K	$C_{p,m}$/J K^{-1} mol^{-1}	T/K	$C_{p,m}$/J K^{-1} mol^{-1}
293.83	1617.2	372.26	2787.3
296.83	1624.8	373.71	2288.6
299.84	1641.2	375.50	2225.2
302.76	1644.5	377.27	2210.8
305.68	1664.8	379.14	2148.3
308.60	1677.1	381.08	2143.7
311.53	1702.7	383.07	2148.9
314.45	1716.0	385.09	2149.6
317.45	1729.3	387.12	2150.3

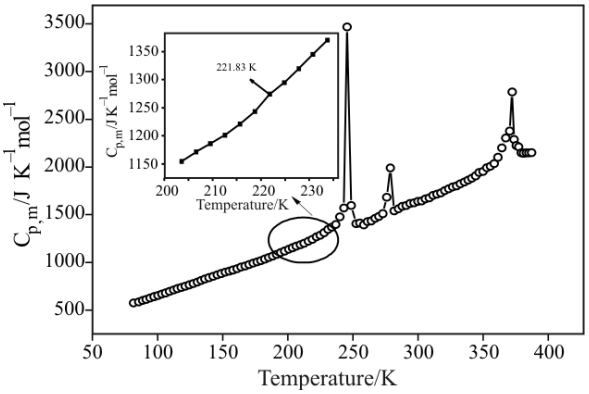

Fig. 1 Experimental molar heat capacities plotted *vs.* temperature of the complex as a function of temperature

Results and discussion

Molar heat capacity, molar enthalpies and entropies

The experimental molar heat capacities of the complex were shown in Fig. 1 and listed in Table 1 from 80 to 390 K.

Figure 1 showed that there is a slight step at 221.83 K and three peaks over the temperature range from 230 to 380 K on the curve. The slight step was due to the glass transition of the complex, which was proved by the DSC test. The peaks from 230 to 380 K were deduced to be the phase transition from 230 to 258 K (T_{trs}=245.45 K), ice point of the free water from 272 to 282 K (T_{trs}=278.69 K), and decomposition of the water from 358 to 380 K (T_{trs}=372.26 K), in the sequence of temperature increment, respectively. The conclusion was made not only experimentially, but also based on the DSC measurement and the documents [17–20].

The temperature, T_{trs}, molar enthalpies, $\Delta_{trs}H_m$, and molar entropies, $\Delta_{trs}S_m$, of the last three-phase transitions from 220 to 258 K, were calculated with the method of diagrammatic area integration and listed in Table 2.

Table 2 Temperature, enthalpy and entropy of the last three phase transitions of the complex obtained from the heat capacity measurements from 80 to 390 K

Transitions	T_{trs}/K	$\Delta_{trs}H_m$/ kJ mol^{-1}	$\Delta_{trs}S_m$/ J mol^{-1} K^{-1}
Glass transition	221.83	–	–
Phase transition	245.46	14.79	60.25
Ice point of water	278.69	1.720	6.170
Decomposition of water	372.26	14.02	37.66

The values of experimental heat capacities in the four regions can be fitted and four polynomial equations were obtained by the least square fitting by using the experimental molar heat capacities ($C_{p,m}$) and the experimental temperatures (T).

- from 80 to 220 K:

$$C_{p,m}/(\text{J K mol}^{-1})=885.92+313.73x-2.302x^2+ +64.415x^3+26.287x^4-39.58x^5 \quad (1)$$

where $x=[(T/\text{K})-150]/70$, x is the reduced temperature and T is the experimental temperature. Correlation coefficient R^2 of least square fitting is 0.9999.

- from 258 to 272 K:

$$C_{p,m}/(\text{J K mol}^{-1})=1441.6+56.838x+67.437x^2- -28.279x^3-95.986x^4 \quad (2)$$

where $x=[(T/\text{K})-265]/7$, its correlation coefficient R^2 is 0.9989.

- from (282 to 358) K:

$$C_{p,m}/(\text{J K mol}^{-1})=1746.1+227.6x+46.246x^2- -14.931x^3+2.6741x^4+33.585x^5 \quad (3)$$

where $x=[(T/\text{K})-320]/38$, its correlation coefficient R^2 is 0.9989.

- from 380 to 390 K:

$$C_{p,m}/(\text{J K mol}^{-1})=2149.6-0.1984x- -0.7675x^2+11.671x^3 \quad (4)$$

where $x=[(T/\text{K})-385]/5$, its correlation coefficient R^2 is 0.9989.

In terms of the polynomials of heat capacity and the thermodynamic relationship, the thermodynamic functions $[H_T-H_{298.15}]$ and $[S_T-S_{298.15}]$ of the complex were calculated in the temperature range from 80 to 390 K with a temperature interval of 5 K and listed in Table 3.

DSC analysis

It can be seen from Fig. 2 that there are three endothermic processes in the temperature range from 150 to 400 K, which is conform to the results of the heat capacity measurement. The temperature ranges and peak values of the three endothermic processes correspond

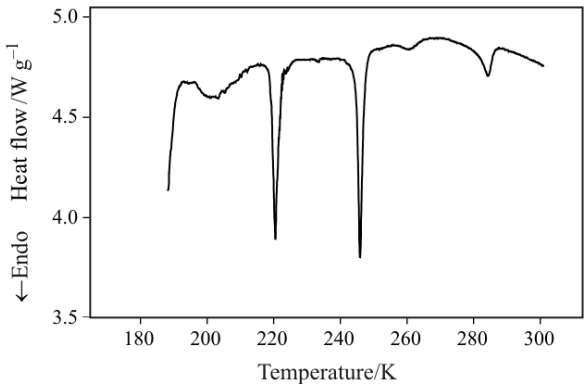

Fig. 2 DSC curve of the complex in the temperature range from 100 to 300 K

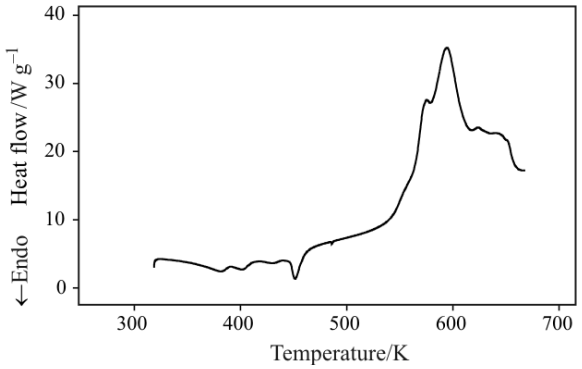

Fig. 3 DSC curve of the complex in the temperature range from 300 to 700 K

to those of the three phase transitions in $C_{p,m}$–T curve obtained from the heat capacity measurements. This result also confirms that there are glass transition and three phase transitions in the temperature range from 150 to 400 K, which include a phase transition, a fusion and a phase transition of the crystal water.

Based on the DSC curve (Fig. 2), the enthalpy and entropy of phase transition of $[Nd(Glu)(H_2O)_5(Im)_3](ClO_4)_6\cdot 2H_2O$ were determined through the method of diagrammatic area integration and listed in Table 4, which were consistent with the values (Table 2) from the heat capacity measurements.

It can be seen from Fig. 3 that there is an exothermic peak on the DSC curve from 550 to 600 K, for the ligand of the complex brake away from the complex.

Glass transition and phase transition

There is a slight step on $C_{p,m}$–T curve (Fig. 1) at 221.83 K and there is a sharp endothermic peak on the DSC curve (Fig. 2) at 221.02 K. The combined consideration of the mechanism of the glass transition, the disappearance of the excess heat capacity and the results of DSC measurement leads to a conclusion that the phase transition is attributed to the glass

Table 3 Thermodynamic functions, $[H_T–H_{298.15}]$ and $[S_T–S_{298.15}]$, of the complex from 80 to 390 K with a temperature interval of 5 K

T/K	$C_{p,m}$/ J mol^{-1} K^{-1}	$(H_T–H_{298.15})$/ kJ mol^{-1}	$(S_T–S_{298.15})$/ J mol^{-1} K^{-1}
80	571.34	–200.41	–1279.9
85	587.91	–197.52	–1244.9
90	607.25	–194.53	–1210.7
95	628.62	–191.44	–1177.3
100	651.38	–188.24	–1144.4
105	675.01	–184.93	–1112.1
110	699.09	–181.49	–1080.2
115	723.31	–177.93	–1048.6
120	747.43	–174.26	–1017.3
125	771.30	–170.46	–986.34
130	794.84	–166.54	–955.64
135	818.03	–162.51	–925.21
140	840.88	–158.37	–895.04
145	863.48	–154.10	–865.12
150	885.92	–149.73	–835.45
155	908.34	–145.24	–806.02
160	930.89	–140.65	–776.81
165	953.71	–135.94	–747.81
170	976.97	–131.11	–718.99
175	1000.8	–126.16	–690.34
180	1025.3	–121.10	–661.82
185	1050.7	–115.91	–633.40
190	1076.9	–110.59	–605.06
195	1103.9	–105.14	–576.75
200	1131.8	–99.551	–548.45
205	1160.4	–93.821	–520.15
210	1189.6	–87.946	–491.83
215	1219.0	–81.925	–463.49
220	1248.5	–75.756	–435.16
225–255	phase transition	–	–
260	1420.73	–68.118	–402.15
265	1441.60	–60.967	–374.91
270	1481.31	–53.638	–347.51
275–280	phase transition	–	–
285	1567.03	–21.042	–72.172
290	1593.33	–13.141	–44.691
295	1616.99	–5.1160	–17.252
298.15	1631.54	0.0000	0.000
300	1640.15	3.0260	10.119
305	1664.13	11.286	37.424
310	1689.65	19.669	64.685
315	1716.99	28.185	91.932
320	1746.10	36.842	119.20
325	1776.82	45.649	146.50
330	1808.98	54.612	173.88
335	1842.62	63.740	201.33
340	1878.08	73.041	228.89
345	1916.24	82.524	256.58
350	1958.60	92.208	284.44
355	2007.48	102.12	312.55
360–375	phase transition	–	–
380	2137.36	291.98	1276.8
385	2149.60	302.72	1304.8
390	2160.31	313.48	1332.6

Table 4 Temperature, enthalpy and entropy of the phase transitions of the complex obtained from DSC measurement from 150 to 390 K

Transitions	T_{trs}/K	$\Delta_{trs}H_m$/ kJ mol^{-1}	$\Delta_{trs}S_m$/ J mol^{-1} K^{-1}
Glass transition	221.02	11.74	53.11
Phase transition	245.76	14.29	58.14
Ice point of water	278.65	1.740	6.140
Decomposition of water	372.26	14.18	38.09

transition. The glass transition was interpreted as a freezing-in phenomenon of the reorientational motion of ClO_4^- ions [17–20].

Based on the same phenomena of heat capacity and DSC measurements, the endothermic process at 245.76 K was deduced to be phase transition. Orientational order/disorder process of perchlorate ion is the origin of the phase transition [17–20].

TG analysis

The TG-DTG curves plotted in Fig. 4 showed that mass loss of $[Nd(Glu)(H_2O)_5(Im)_3](ClO_4)_6{\cdot}2H_2O$ began at about 297 K and ended at about 670 K, and the whole process were divided to three stages. The mechanism of the decomposition was deduced to be as follows:

$$[Nd(Glu)(H_2O)_5(Im)_3](ClO_4)_6{\cdot}2H_2O \rightarrow \rightarrow [Nd(Glu)(H_2O)_5(Im)_3](ClO_4)_6$$

$$[Nd(Glu)(H_2O)_5(Im)_3](ClO_4)_6 \rightarrow Nd(ClO_4)_6 \rightarrow NdO_{3/2}$$

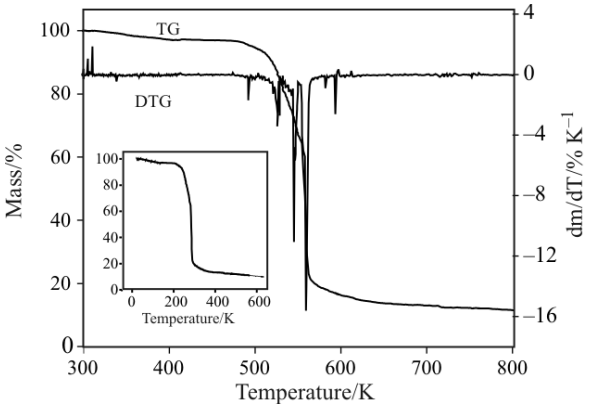

Fig. 4 TG-DTG curve of the complex

Conclusions

In the present work, a complex, $[Nd(Glu)(H_2O)_5(Im)_3](ClO_4)_6{\cdot}2H_2O$, which has never been reported, was synthesized and characterized. The thermodynamic properties of the complex were studied by the adiabatic calorimetry and the DSC technique. Glass transition and phase transition were discovered at 221.83 and 245.45 K, respectively. The glass transition was interpreted as a freezing-in phenomenon of the reorientational motion of ClO_4^- ions and the phase transition was attributed to the orientational order/disorder process of ClO_4^- ions. The heat capacities of the complex were measured with the automatic adiabatic calorimeter and the thermodynamic functions $[H_T–H_{298.15}]$ and $[S_T–S_{298.15}]$ were derived in the temperature range from 80 to 390 K with temperature interval of 5 K. Thermal decomposition behavior of the complex in nitrogen atmosphere was studied by TG and DSC.

Acknowledgements

This work was financially supported by the National Nature Science Foundation of China under the grant NSFC No. 20373072, 20753002.

References

1 Z. P. Zheng, Chem. Commun., 24 (2001) 2521.
2 H. Xu and L. Chen, Spectrochim. Acta Part A, 59 (2003) 657.
3 X. Q. Wang, T. Z. Jin and Q. R. Jin, G. X. Xu, Polyhedron, 13 (1994) 2333.
4 T. Glowiak, J. Legendziewicz, E. Huskowska and P. Gawryszewska, Polyhedron, 15 (1996) 2939.
5 L. Csöregh, P. Kierkegaard, J. Legendziewicz and E. Huskowska, Acta Chem. Scand., Ser., A41 (1987) 453.
6 X. Z. Lan, Z. C. Tan, B. P. Liu, Z. D. Nan, L. X. Sun and F. Xu, Thermochim. Acta, 416 (2004) 55.
7 B. P. Liu, Z. C. Tan, J. L. Lu, X. Z. Lan, L. X. Sun, F. Xu, P. Yu and J. Xing, Thermochim. Acta, 397 (2003) 67.
8 K. Nakamoto, Infrared Spectra of Inorganic and Coordination Compounds, 4th Ed. John Wiley & Sons Inc., New York 1986, p. 258.
9 A. L. Wayda and M. L. Kaplan, Lyons. Polyhedron, 9 (1990) 751.
10 Z. C. Tan, G. Y. Sun, Y. Sun, A. X. Yin, W. B. Wang, J. C. Ye and L. X. Zhou, J. Thermal Anal., 45 (1995) 59.
11 Y. J. Song, Z. C. Tan, S. W. Lu and Y. Xue, J. Therm. Anal. Cal., 77 (2004) 873.
12 Z. D. Nan and Z. C. Tan, J. Therm. Anal. Cal., 76 (2004) 955.
13 S. X. Wang, Z. C. Tan, Y. Y. Di and F. Xu, J. Therm. Anal. Cal., 76 (2004) 335.
14 F. Xu, L. X. Sun, Z. C. Tan, J. G. Liang, Y. Y. Di, Q. F. Tian and T. Zhang, J. Therm. Anal. Cal., 76 (2004) 481.
15 B. Xue, J. Y. Wang, Z. C. Tan, S. W. Lu and S. H. Meng, J. Therm. Anal. Cal., 76 (2004) 965.
16 D. G. Archer, J. Phys. Chem. Ref. Data, 22 (1993) 1441.
17 M. M. Anna, M. Edward, Ł. Hetmańczyk, I. Natkaniec, E. Ściesińska, J. Ściesiński and S. Wróbel, Chem. Phys., 317 (2005) 188.
18 S. S. Hangam and E. R. Westrumj, Thermodyn. Properties Globular Mol., 64 (1960) 1547.
19 Y. Yukawa, S. Igarashi, Y. Masuda and M. Oguni, J. Mol. Struct., 605 (2002) 277.
20 A. A. Udowenko, N. M. Laptash and I. G. Maslennikova, J. Fluorine Chem., 124 (2003) 5.

DOI: 10.1007/s10973-008-9243-4